Preprints.org

Article

The Symbiotic Organ of *Xyleborus* Ambrosia Beetles: Cell Structure of the Preoral Mycangia Housing Partner Symbiotic Microbes

Ross A. Joseph , Esther Tirmizi , Abolfazl Masoudi , Nemat O. Keyhani [*]

Article

The Symbiotic Organ of *Xyleborus* Ambrosia Beetles: Cell Structure of the Preoral Mycangia Housing Partner Symbiotic Microbes

Ross A. Joseph †, Esther Tirmizi †, Abolfazl Masoudi and Nemat O. Keyhani *

University of Illinois at Chicago, Chicago, Illinois, 60607

* Correspondence: keyhani@uic.edu

† These authors contributed equally to this work.

Simple Summary: Fungal farming insects, which include certain species of ants, termites, beetles, and others, have independently evolved the unique ability to grow their own food. Ambrosia beetles represent one such group of insects, which grow their fungal partners as food within galleries that they construct within their tree habitats. The beetles maintain their galleries and tend their fungal "crops" as the sole source of food for larvae and adults. This association is so important to the beetles that they have evolved structures (termed mycangia) on their bodies used to house a small amount of the fungus to use as "seeds" for maintaining and/or initiating new colonies. Here, we characterize the morphology and cellular structures that comprised the mycangia of *Xyleborus* ambrosia beetles. We show that the mycangia in these beetles are pouch-like and include specialized cellular walls and other layers that comprise their boundaries, with a series of projections into each mycangium, and long comb-like spines that may function as gates into and out of the mycangia. Our data provide a model for the dynamic nature of this unique organ.

Abstract: Ambrosia beetles have evolved specialized structures termed "mycangia", which are used to house and transport partner symbiotic microbes. Microbial partners include at least one obligate mutualistic filamentous fungus used as food for larvae and adults and potentially secondary filamentous fungi, yeasts, and bacteria, although the roles of these secondary partners remain poorly understood. Beetles in the genus *Xyleborus* possess a set of two pre-oral mycangial structures located within the head on either side of the mouth parts/mandibles. These mycangia develop in pupae, with newly emerged adults acquiring partners from the environment. However, information concerning the cellular structure and function of the *Xyleborus* mycangia remains limited. We show that the mycangia are lined with a thick layer of striated dense material, followed by layers of insect epithelial cells, with different types of spine-like structures directed into the mycangia. Larger (5-10 µm) Ross projections were concentrated within and near the entrance of the mycangia, with smaller tubules and filaments (4-8 µm) within the mycangia itself. In addition, rows of "eyelash" structures were seen lining the inside of mycangia, with the fungal cells apparently free-floating within the mycangial enclosure or in close association with projections. Serial sections revealed nearby mandible articulations, eyes and antennae, and mandibular, pharyngeal, and labial muscles, along with the mycangial entry/exit channel leading into the pre-oral cavity. Sheets of comb-like large spines at the mycangial entrance and opposite the mycangia attached to the roof of the labrum or epipharynx were noted that may serve as an interlocking mechanism for opening/closing the mycangia and for guiding fungal cells into entry/exit channels. In addition, mandibular fibra (muscle tissue) potentially enervating and affecting the mechanism of mycangial functioning, i.e., acting to fill/empty the mycangia were noted. These data support the hypothesis that the twin pre-oral mycangia in *Xyleborus* beetles are dynamic organs with evolved specialized cellular structures that mediate their function in housing and dispensing partner microbial symbionts.

1. Introduction

The term "ambrosia beetle" describes a convergent lifestyle rather than a phylogenetic designation, where disparate beetle lineages have "domesticated" equally diverse genealogies of partner fungi [1–3]. Typically, less than the size of a grain of rice, these small beetles bore into the sapwood of trees where they excavate galleries to rear their brood, with different species showing variations in degree of sociality [1,4]. Invasion of ambrosia beetles into new habitats, facilitated in part by transport of trees and lumber, can have profound effects on indigenous ecosystems, not only in terms of vectoring plant pathogens, but also on wood decay and turnover [5–10]. The beetles do not feed directly on tree components but rather cultivate their fungal partners along verdant walls of their galleries, often producing swollen, tender conidiospore-like cells upon which larvae and adults feed [11–15]. For ambrosia beetles, at least one fungal partner has become obligate. Via the process of this co-adaptation and evolution, likely over a span of tens to several hundred million years in some instances, the beetles have evolved specialized structures on or in their bodies, termed mycangia, to house and transport their fungal partner(s) [16–19]. Due to the polyphyletic nature of this adaptation, varied ambrosia beetle lineages have evolved completely different mycangia. Some mycangia are dorsal/pronotal pits and/or consist of elytral notches, whereas others include prothoratic tubes, mesonotal pouches, setose patches, prothoractic cavities, and preoral pockets/organs, the latter within the head of the beetle, around the mouthparts/mandibles [20].

Pre-oral mycangia are typically found in pairs inside the head, flanking the mouthparts and near the alimentary canal. From current descriptions, most ambrosia beetles that contain pre-oral mycangia belong to the subfamily Scolytinae, and are found in the Ipini, Xyleborini, and Xyloterini tribes, although, as mentioned, different genera within these tribes may have divergent mycangial structures, and examples of pre-oral mycangia can be found beyond these beetles [20]. Overall, structural and functional aspects of most mycangia remain significantly understudied, however, important insights have been gained in several exemplars. The pleural cavities found in adult *Trypodendron* (Xyloterini) are lined with gland cells that are activated when partner fungi enter, resulting in a milieu that favors selective propagation of the symbiont [21]. When the beetle, carrying its fungal inoculum, reaches a host tree, fungal cells are released during colony excavation and the mycangia (gland cells) begin to deteriorate. As can be expected, structure-function in other types of mycangia can be radically different. Sectioning and histological staining of pre-oral mycangia in *Euwallacea*, *Ambrosiodmus*, *Premnobius*, and *Xyleborus* beetles [17,22], has helped define ultrastructural aspects of these mycangia revealing their shape, size, anatomical location, and connection to the foregut or pre-oral cavity. Non-invasive, micro-computed tomography (µCT) has also been used to visualize the pronotal (*Euplatypus*, *Scolytoplatypus*), mesonotal (*Xylosandrus*), and oral (*Ambrosiophilus*, *Euwallacea*) mycangia of a variety of beetles [17]. The dual pre-oral mycangia of *Euwallacea* beetles have been visualized by µCT across development and between sexes [23,24]. These latter data have shown the potential presence of numerous pre-oral mycangia in *Euwallaceae* beetles (superior and inferior mycangia), their development during pupation, and that, as adults, these structures appear fully "inflated" in the absence of colonizing fungal partners, in contrast to the mesonotal mycangia of *Xylosandrus* beetles, which have been shown to inflate upon exposure to partner fungi and deflate following their expulsion.

Xyleborus beetle species include invasive members whose fungal partners are highly destructive fungal tree pathogens [2,25]. *Xyleborus glabratus* is one such invasive species in the United States, and its fungal symbiont, since named *Harringtonia lauricola*, is the causative agent of laurel wilt, a disease that has killed hundreds of millions of redbay, swamp bay, and sassafras trees, and now threatens the avocado industry in the United States [26–28]. *H. lauricola* has now been isolated from environmental samples of indigenous *Xyleborus* beetles, including *X. affinis*, and the ability of these latter beetles to maintain *H. lauricola* as their major symbiont has been confirmed in the laboratory [26,29,30]. These beetles have dual pre-oral mycangia located within the head, just behind and

beneath the mandibles [30]. *Xyleborus* beetles can harbor fungal species now separated into the *Raffaelea, Harringtonia,* and *Dryadomyces* genera (all previously characterized as *Raffaelea*), as well as limited colonization by *Neocosmospora* (previously *Fusarium*) [14,31,32]. Mycangial colonization of *X. affinis* has been probed using fungal strains transformed to express reporter (eGFP and RFP)-marker genes [30]. These data showed stability to starvation as well as dynamic turnover, and transmission electron microscopy (TEM) showed a dimorphic shift in the growth of the fungus in the mycangia. *X. affinis* has been shown to be a good host for *H. lauricola*, with the related beetle species, *X. ferrugineus* colonized to a considerably lower extent, indicating variation in colonization capacity between even closely related beetle species. Here, we focus on structural and cellular aspects of the *Xyleborus* pre-oral mycangia, defining different morphological features that support the hypothesis of the mycangia being highly evolved organs lined by host cells and diverse structures, with specific structures that may contribute to partner selection, entry/exit, and/or fungal cell retention and maintenance within the mycangia. Our data indicate the potential for specific muscle fibers (termed mandibular fibra) and specialized comb-like spines that may act in concert with mandibular movements to regulate the functioning of the mycangia as symbiotic fungal transport organs.

2. Materials and Methods

2.1. Insect Rearing, Fungal Strains, and Culture Conditions

Xyleborus affinis colonies were maintained under laboratory conditions, and aposymbiotic beetles were reared for colonization experiments as previously described [30]. Briefly, sawdust agar medium was made by mixing 60 g wood flour, 15 g coarse sweetgum sawdust, 20 g agar, 10 g sucrose, 5 g corn starch, 5 g casein, 5 g yeast extract, 1 g Wesson salt mixture, and 2.5 mL wheat germ oil into 500 mL of water. Following autoclaving and cooling, 350 mg streptomycin and 10 mg tetracycline were suspended in 5 mL 95% ethanol and added to the mixture. Roughly 15-20 mL of this mixture was added to 50 mL tubes. Colonies were initiated using 3-15 female beetles and 1-3 male beetles, and tubes were maintained with caps loosely tightened for 25-30 days in the dark at 23-25°C. Colony tubes are carefully dissected to remove adult beetles, pupae, and larvae, with adult beetles used to initiate new colonies. Pupae and larvae were separated, surface sterilized with 70% ethanol and three washes with sterile distilled water, and maintained on sterile, moistened filtered paper until adult beetles emerged to generate aposymbiotic beetles for colonization assays. Fungal strains of *Harringtonia lauricola*, including those transformed to express green- or red-fluorescent protein (GFP/RFP), have been previously described [33], and unless otherwise noted, were routinely grown on potato dextrose agar (PDA) for use.

2.2. Microscopy

To obtain microscope images of fungal cells within *X. affinis* mycangia, aposymbiotic beetles were colonized using GFP-expressing *H. lauricola* as above, embedded in Optimal Cutting Temperature (OCT) mounting medium, and frozen in a bath of isopentane cooled in liquid nitrogen. Frozen blocks were then sectioned using a Leica 3050S cryostat (Leica, Wetzlar, Germany) to a thickness of 5-20μm. Sections were then collected directly onto microscope slides, followed by fixation in 4% PFA for 20 minutes and three washes in sterile distilled water for three minutes each to remove PFA and OCT. Slides were then dried and mounted in Vectashield hardset mounting medium containing DAPI and phalloidin (Vector laboratories, Plain City, OH) for fluorescent staining of nuclei and actin filaments, respectively. Mounted sections were then visualized using a Keyence BZX-800 fluorescence microscope at 40x, 60x, and 100x objective magnification using brightfield, TRITC, GFP, and DAPI fluorescent channels. For fluorescent images, Z stacks were collected over a range encompassing the signal and assembled into a full focus image in the Keyence BZX-800 Analyzer software, while for brightfield photos, single images were taken and overlayed with full-focus fluorescent images. Transmission electron microscopy (TEM) images were obtained

as previously described [30]. Measurements of anatomical structures from microscopy images were obtained using ImageJ software (National Institutes of Health, Bethesda, MD, USA).

3. Results

3.1. Mandible, Muscle, and Cross-Section Analyses of the X. affinis Mycangia

X. affinis larvae, pupae, and adults are ~1.5, 2, and 2.1 mm in length (Figure 1A–C). Larvae pass through three instars, with adults emerging from pupae after 6-7 d. On adults, deeply emarginate compound eyes, located on either side of the mandibles, encompassed upper (~140x140 µm) and lower (~170x140 µm) patches of ommatidia containing the cornea, cones, and photoreceptor cells, with the small club-foot antennae characteristic of ambrosia beetles adjacent (Figure 1D,E). Mandibles (~150-200 µm) were located above the submentum and were multidentate and surrounded by dense setae (Figure 1E–G).
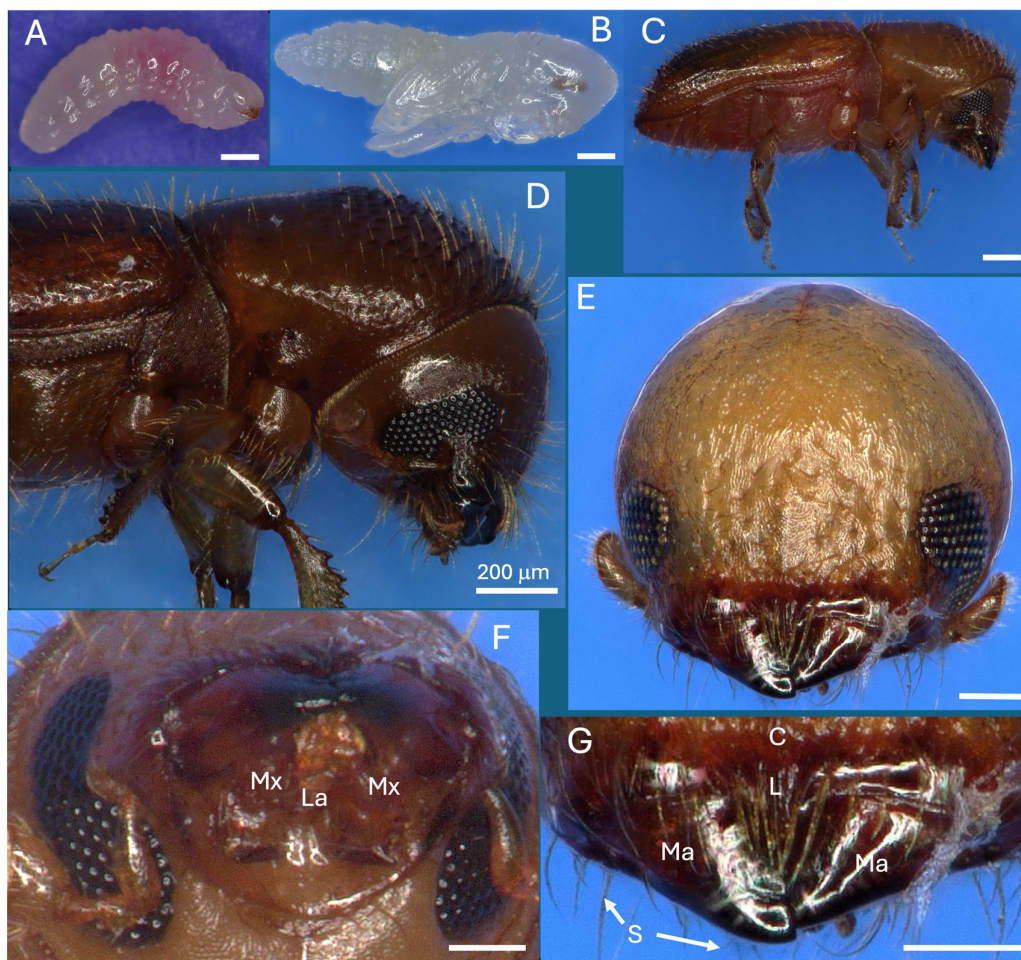

Figure 1. *X. affinis* life stages, head anatomy, and mouth parts. (A) Larva, (B) pupa, (C) adult, (D) adult sideview, (E) head, frontal view, (F) mandibles and maxillae, bottom view, (G) mandibles, top view. Scale bars: (A)-(D) = 200 mm, (E)-(G) = 100 mm. Abbreviations are as follows: Mx = maxillae, La = labium, Ma = mandibles, S = setae, L = labrum, C = clypeus.

Longitudinal cross-sectioning of whole adult female beetles revealed mycangia, gut tract, ganglia, and musculature, with significant mandibular muscles apparent extending from the head to the jaws (Figure 2A,B). A corresponding cross section stained with DAPI and phalloidin and visualized via fluorescence microscopy revealed the major organs of the beetle including the brain, hindgut, posterior-, and anterior-midguts, as well as proventriculus and crop (Figure 2C). Near/at

the head region, the labial, pharyngeal, and mandibular muscles were also apparent (Figure 2C,D). In addition, strongly phalloidin-staining mandibular fibra, immediately adjacent (slightly above) the mycangia, were seen. As the beetle was fed a partner symbiotic fungus (*H. lauricola*) expressing RFP as detailed in the Methods section, fungal cells within the mycangia could be detected via fluorescence microscopy. These cells were seen to localize exclusively to mycangia following colonization, indicating that host beetles can employ efficient mechanisms to guide partner fungal cells into mycangia and store them there without persistence of cells in surrounding insect anatomical structures.
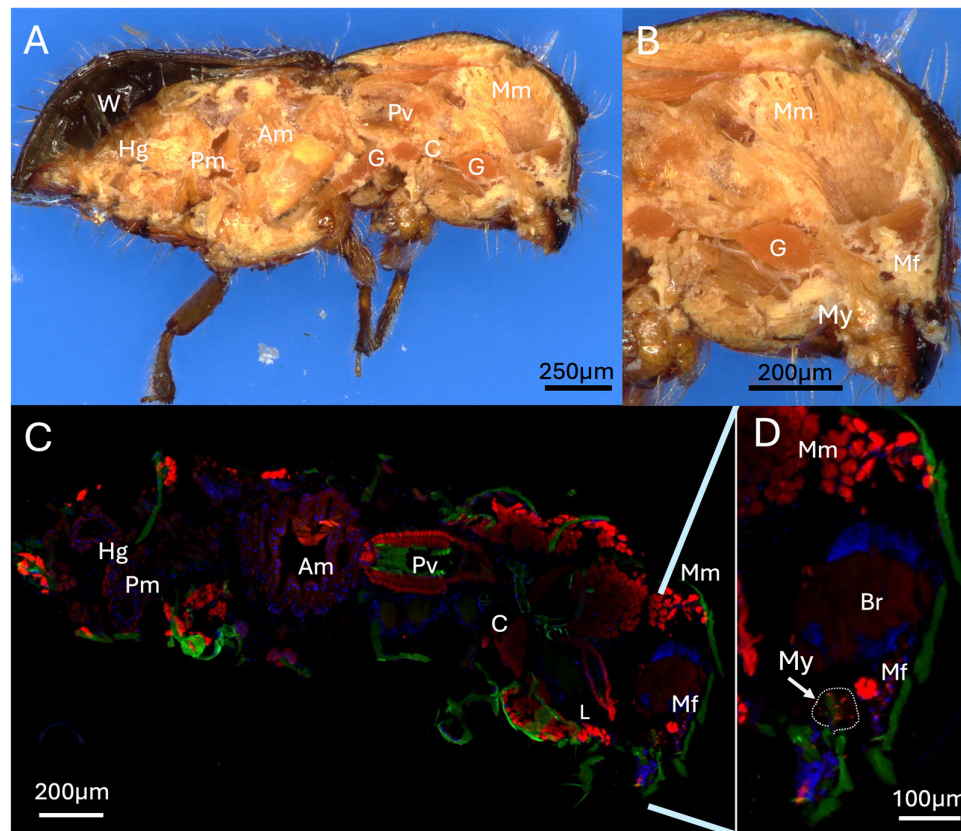

Figure 2. Longitudinal section of whole adult female beetle (A & B), examined via dissecting microscope, (C & D) fluorescent microscopy after DAPI nuclear and phalloidin (actin) staining. Abbreviations: W = wings, G = ganglia, Hg = hindgut, Pm = posterior midgut, Am = anterior midgut, Pv = proventriculus, C = crop, L = labial muscle, Mm = mandibular muscle, Mf = mandibular fibra, Br = brain, My = mycangia (circled).

Using RFP- and eGFP-labeled *H. lauricola* to mark the mycangia, a series of lateral cross-sections (20 µm, see inset in figure) of the mouthpart region revealed colonization of twin pre-oral mycangia (Figure 3A–D). In the foremost section, mandibular articulations and muscles could be discerned, showing that these articulations sit directly in front of, and connect to, the mycangia via the chitinous lining of entry/exit canals (Figure 3A). Both mycangial pouches could be seen emerging in the next two sections with the antennae, eyes, and esophagus also apparent (Figure 3B,C), with the fourth section likely exposing the outer posterior edge of one of the mycangial organs (Figure 3D). This posterior edge appeared as a thin translucent membranous layer textured by rows of small projections ordered neatly across the interior surface of this structure.
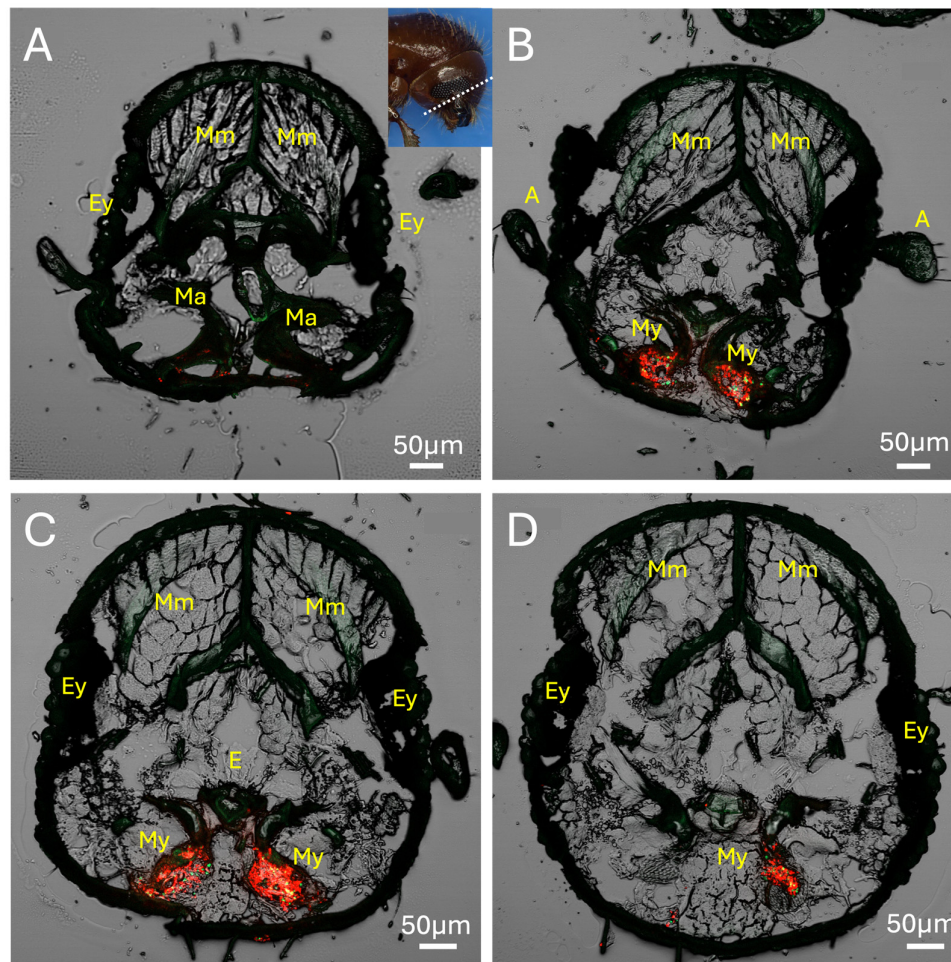
Figure 3. (A-D) Series of four serial sections through *X. affinis* head showing mandible articulations (Ma), mycangia (My), eyes (Ey), esophagous (E), antennae (A), mandibular muscles (Mm), pharyngeal muscles, labial muscles. Beetle was colonized with GFP- and RFP-expressing *H. lauricola* cells, showing localization within mycangia. Note: Image in panel C republished with permission from [30].

Further representative sections immediately within the mouthparts revealed connection of mandibular muscles to the mandibular/mycangial articulations, as well as outlines of entry/exit channels, which appeared as dense masses of melanized/sclerotized tissue with a furrow leading from the pre-oral cavity to the interior of the mycangia (Figure 4). The mycangial organs themselves were irregular in shape and frequently with a pinched lateral end opposite the entry/exit canal. This furrowed end was more frequently noted in later serial sections and appears to be a feature of the dorsal section of the mycangia, situated in the rear-most portion further from the mandibles (see also Figure 8B) and surrounded by a dense striated layer of tissue which may potentially function to contract and squeeze the mycangium, aiding in expulsion of fungal cells during inoculation of fungal gardens along gallery walls. As these beetles were fed a mixture of RFP- and eGFP-expressing *H. lauricola* fungal symbiont partner cells, both green and red-fluorescent signals corresponding to the fungus could be discerned, showing robust colonization within the mycangial compartments. Almost all fungal cells noted in these, and subsequent analyses (and images) shown below, appeared to be single-celled blastospore/yeast-like cells apparently freely floating within the mycangia or in close association with spine-like projections along the inner mycangia lumen walls.
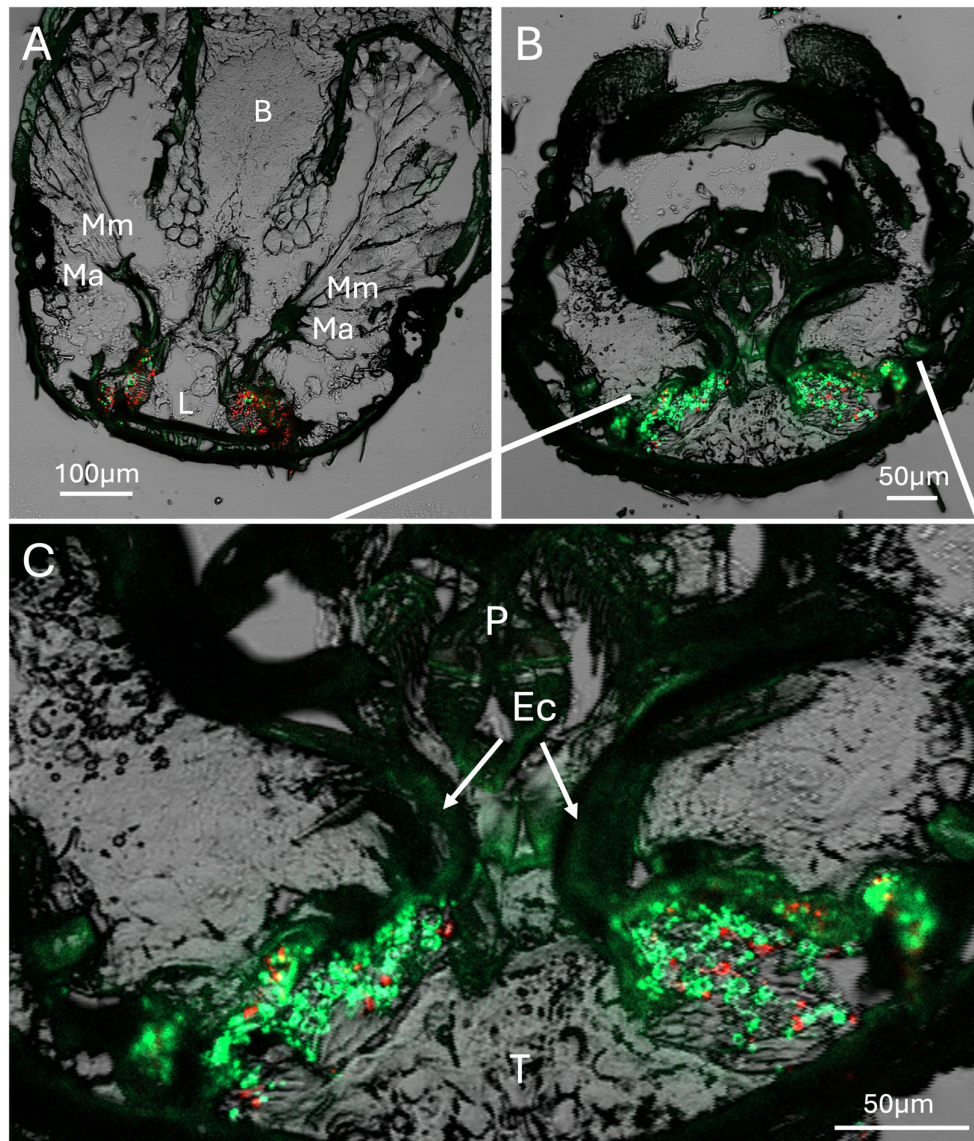
Figure 4. Sections showing head anatomy, including mycangia and mouthparts in more detail. (A) Section showing connection of mandibular muscles (Mm) to mandibular/mycangial articulation (Ma), brain (B), and labium (L). (B) Posterior section showing colonized mycangia with pinched ends (C) Close-up detail of twin pre-oral mycangia. Ec = entry/exit channel, P = pharynx, T = tubular tissue region.

In addition to the mycangia colonized by fungal cells, signals (of eGFP-expressing fungal cells) could be seen within the entry/exit channels, as well as occasionally within the esophagus of the beetle, apparently denoting beetles which were frozen for cryosectioning while in the process of eating fungal cells (Figure 5). In these, and previous sections shown, a clear sclerotized host structure could be discerned surrounding mycangial pouches, particularly in anterior sections closer to the mandibular articulations (Figure 5C, marked with a dashed red line around one of the mycangial pouches).
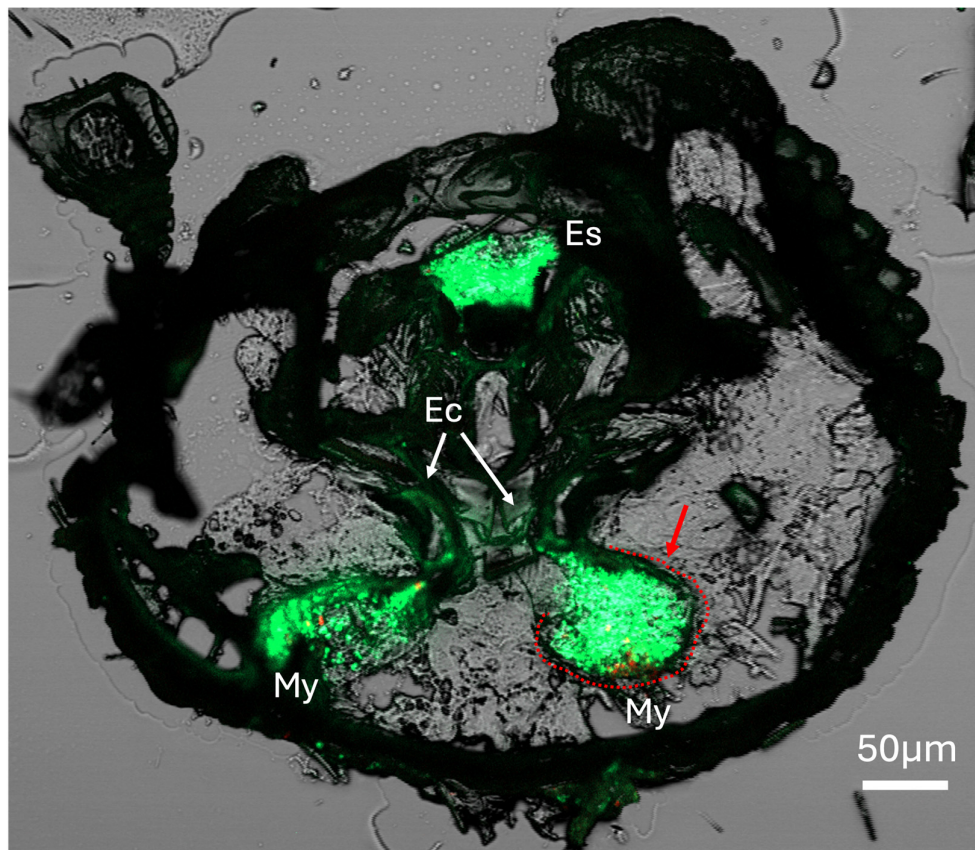
Figure 5. *X. affinis* beetle fed on fluorescent protein-expressing fungal cells showing localization of fungal cells to mycangia and entry/exit canals, as well as fungal cells within the esophagus of the beetle. Red arrow and dashed line indicate a sclerotized structure outlining the mycangium. My = mycangium, Ec = entry/exit channel, Es = esophagus.

Finer Details of Surrounding External and Internal Structures of the Mycangia

Epifluorescence microscopy of the area immediately surrounding the mycangia revealed the hypopharynx and mandibular articulations above and adjacent to the mycangial pouches (Figure 6). Upper and lower sets of large spines (Ls) at the entry/exit channels (Ec) were noted which may guide fungal cells into mycangia and assist in their retention. Beneath and between mycangia, clusters of tubules were noted. In addition, Ross projections (Rp) along a portion inside the mycangia, as well as rows of "eyelash" projections (Ep) lining the inside, were seen.
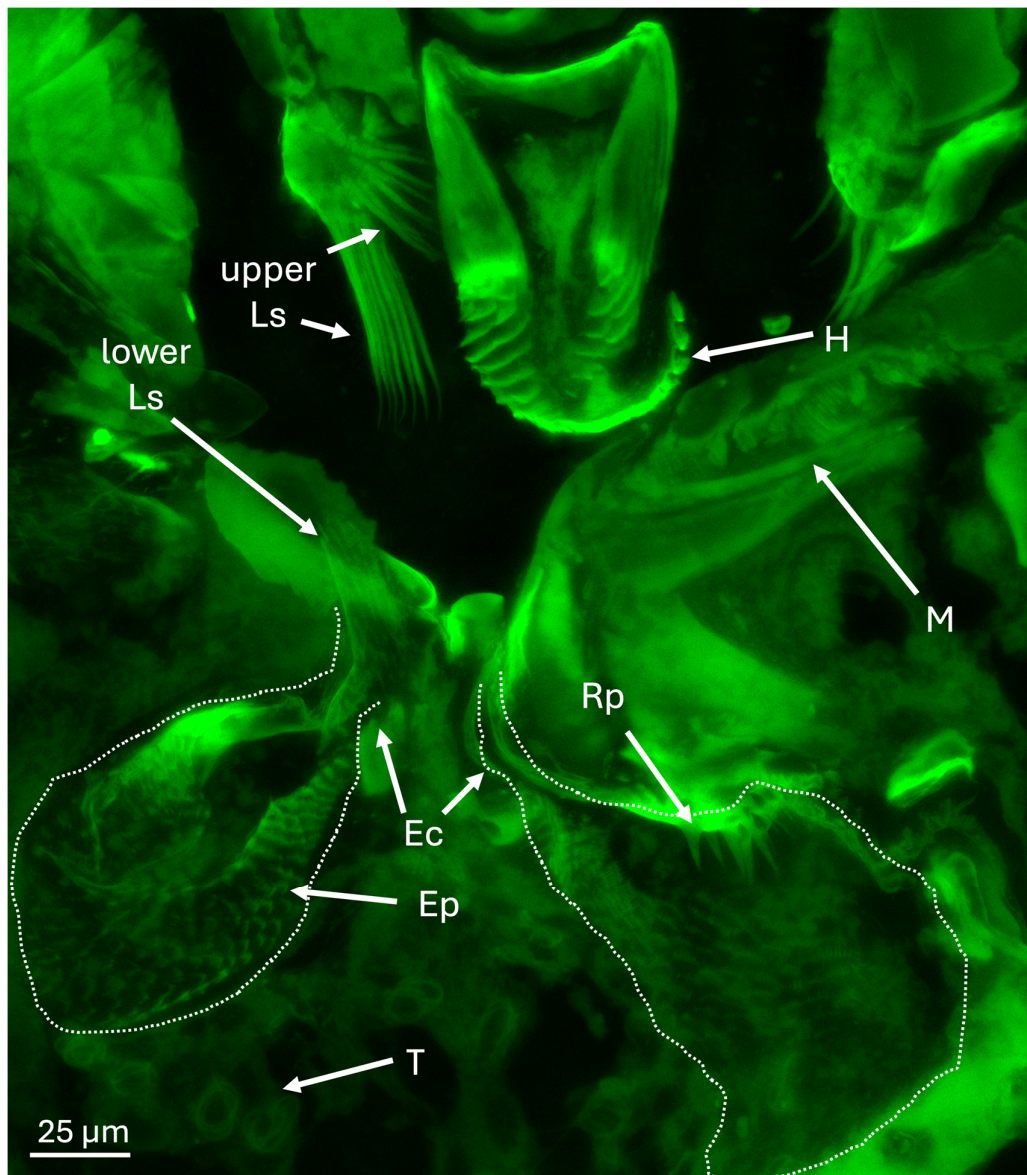
Figure 6. Epifluorescence image showing mouthparts and mycangia (dashed lines), including Ross projections (Rp), eyelash projections (Ep), entry/exit channels (Ec), hypopharynx (H), mandible (M), putative tracheoles (T), and upper and lower large spines (Ls) at entrance to mycangia and opposite in pre-oral cavity.

Sections stained with DAPI revealed that the mycangia is surrounded by a dense layer of cells with small nuclei that extend into the surrounding tissues, with insect cells becoming more spaced apart further away from the mycangia and the nuclei becoming larger, with the tubular region between and below mycangia characterized by distinct large and spaced apart nuclei (Figure 7A,B), with higher magnification brightfield and fluorescence images showing the entry/exit channel, fungal cells within the mycangia, and rows of eyelash projections and intermediate projections (Figure 7C,D).
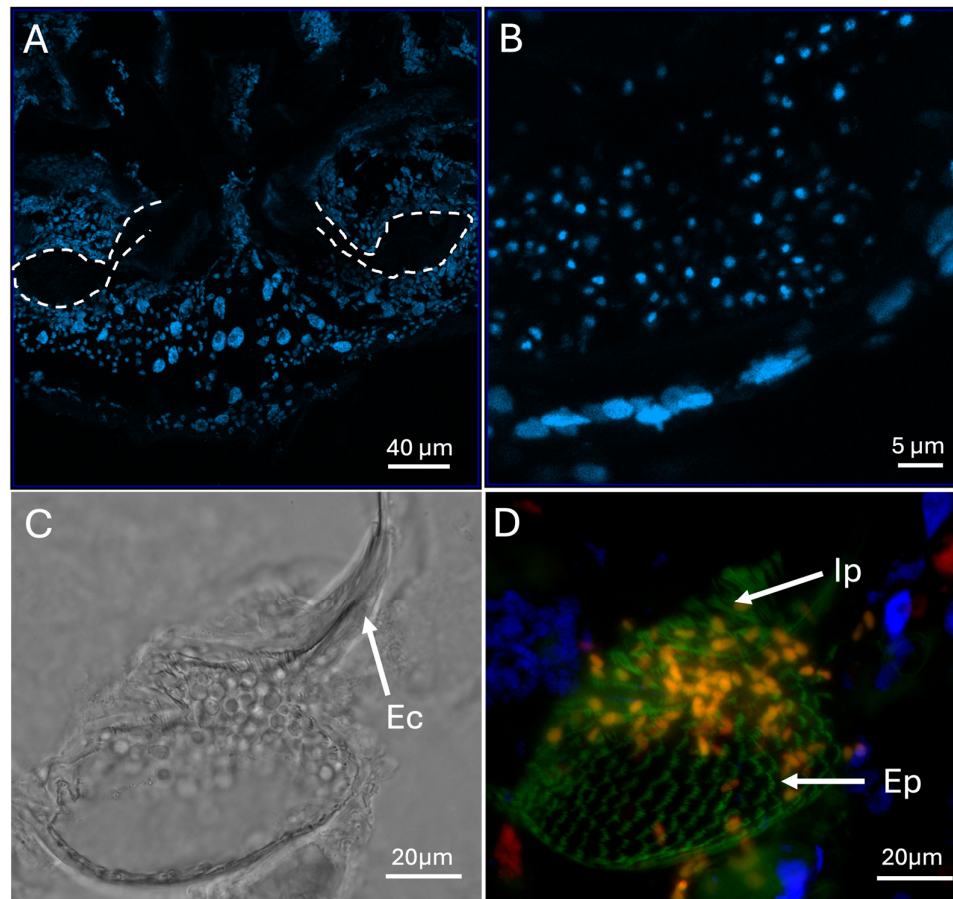
Figure 7. (A - B) DAPI-stained mycangial sections showing host cells surrounding the organ. (C) Bright field and (D) fluorescence images of mycangia and entry/exit channel (Ec), "eyelash" projections (Ep) and intermediate projections (Ip) lining the mycangia. Fungal cells can be seen within the mycangia in the bright field and are orange in the fluorescent image.

The entry exit channel appeared to have a wider (11-14 µm) initial region that narrowed to 1-5 µm, with Ross projections apparent near the entryway, which gave way to smaller intermediate- and eyelash-projections forming a surrounding layer within the mycangia (Figure 8A,B). Columns of striated tissues potentially corresponding to skeletal-like muscle were also seen near the beginning of the entry channel, and fungal cells were readily apparent within the mycangia.
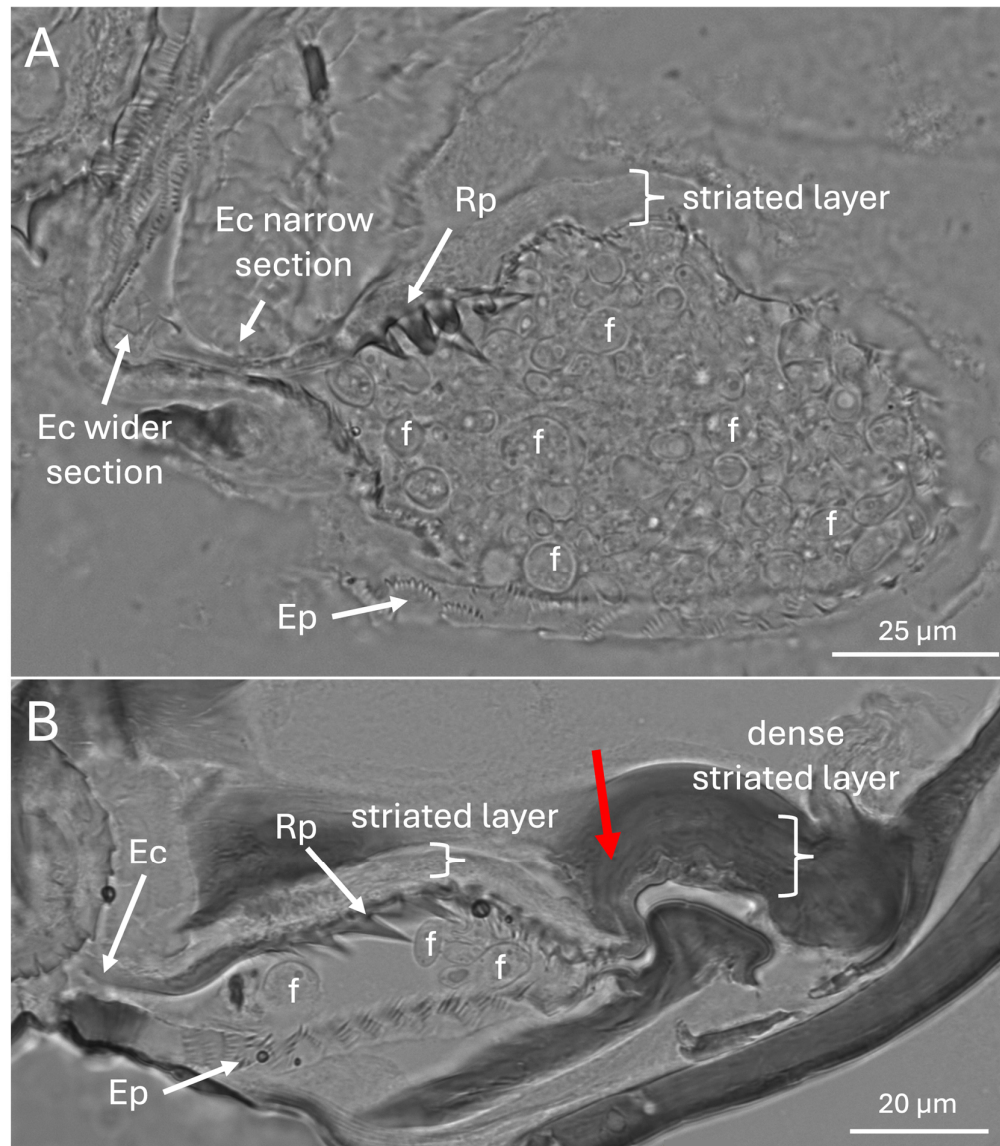
Figure 8. (A & B) Brightfield images showing Ross projections (Rp), eyelash projections (Ep), entry/exit channel (Ec), and fungal cells (f). Note mycangia in (A) is full of fungal cells, only some labeled with an "f". In panel B, the posterior invagination of the mycangia is marked with a red arrow.

To further explore any muscle structures near the mycangia, sections were stained with phalloidin and counterstained with DAPI. Fluorescent microscopic images showed the clear outlines of the mycangia (containing eGFP-expressing fungal cells), surrounded by host cells with two sets of brightly phalloidin staining striated (muscle) structures on the sides of each mycangium, one set at the peripheral boundary of the mycangia and one just above each mycangium separated by a layer of dense DAPI-staining tissue (Figure 9A). These muscular structures on the peripheral boundaries (furthest from the entry/exit channels and esophagus) consist of 8-10 tightly bundled sets of fibers immediately adjacent to mycangia, while those above mycangia and bordering dense DAPI-staining tissues appear to consist of 2-3 brightly phalloidin-staining bundles. Striations in these muscle tissues ran parallel to or slightly angled from the walls of the mycangia. Higher magnification images, including epifluorescence images, revealed bundles (3-5) of columnar striated staining characteristic of skeletal muscle tissues at the periphery of the mycangia (Figure 9B,C).
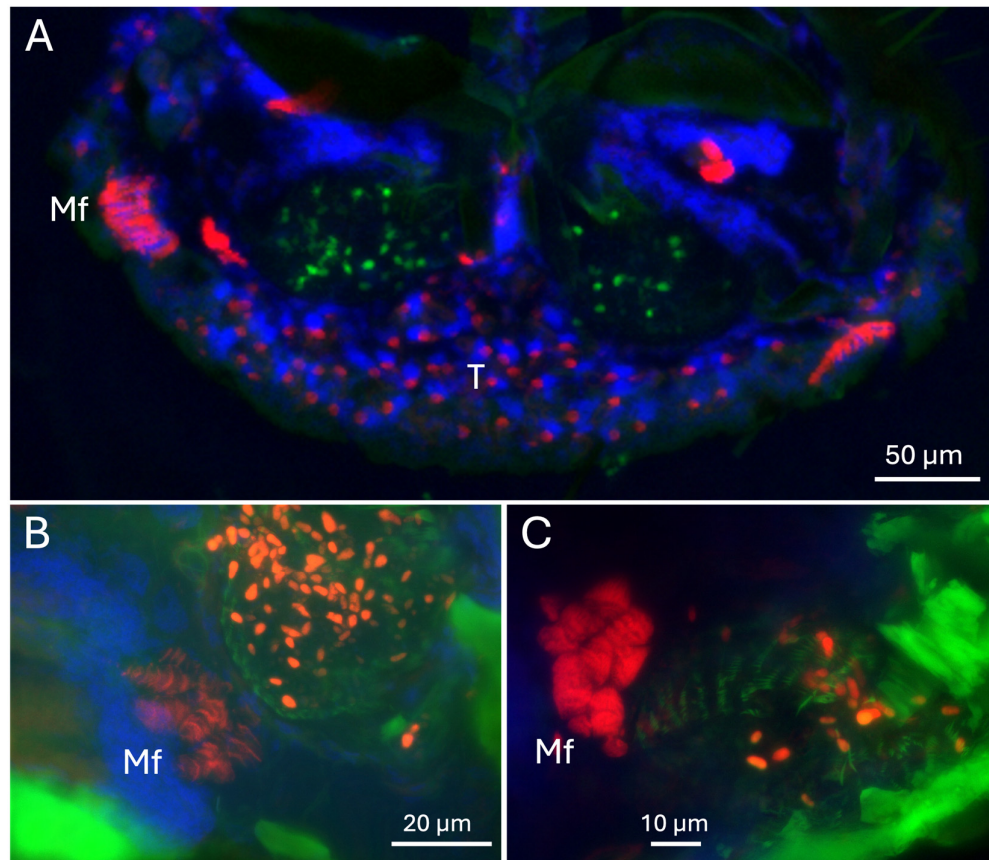
Figure 9. (A-C). Mf = mandibular fibra. T = tracheolar region showing large DAPI-staining nuclei and numerous punctate phalloidin-staining points.

TEM of cross sections of the mycangia revealed a layer of striated material surrounding the mycangium (Figure 10A,B). Ross projections, as well as smaller projections directed into the mycangia containing fungal cells, were also seen. The TEM images confirmed that most fungal cells within the mycangia displayed a free-floating yeast or blastospore-like growth morphology with variations in size and shape observed, as well as evidence of budding growth (red arrows, Figure 10C,D). Both short, and longer Ross projections appeared to have a dense (in relation to the inside of the mycangia) layer, which itself was surrounded by a layer of nucleated host cells, which gave way to the surrounding rings of dense tissue (striations). Thus, the inner lining of the mycangia containing the short and longer Ross projections consisted of a layer (~1-1.5 µm) of dense material (mycangial cuticular layer) surrounded by an outer (in relation to the mycangia) layer or mycangial epithelium comprised of host cells (Figure 10E,F). The longer intermediate and/or Ross projections (e.g., extending ~ 6-10 µm in Figure 10B) appeared to consist of an extension of the mycangial cuticular layer, with nucleated host cells at its base. A summary model of the features of the *Xyleborus* mycangia is given (Figure 11).
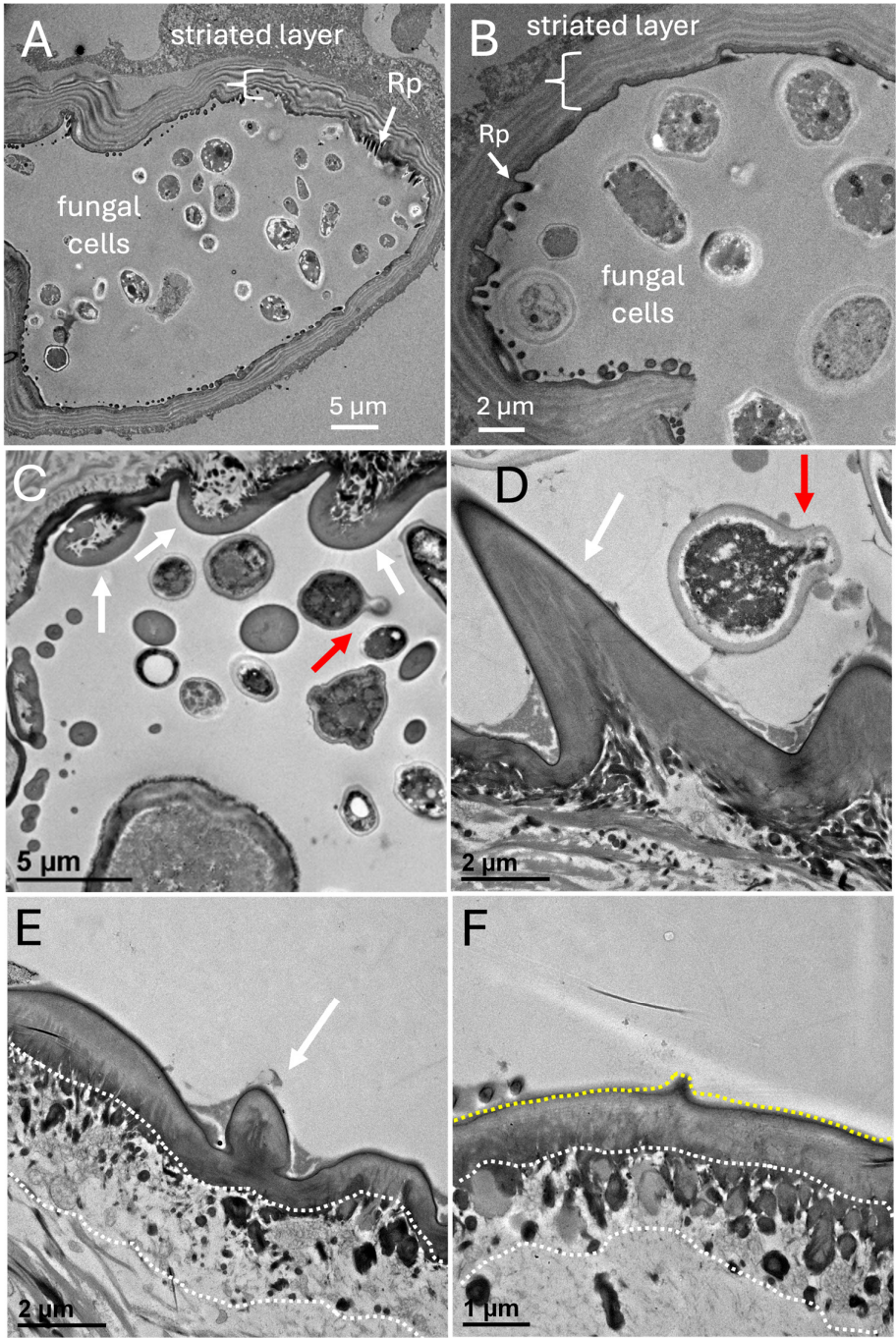
Figure 10. (A-F) TEM cross sections of various projections (red arrows) in *X. affinis* pre-oral mycangia, f = fungal cell, epithelial layer (white dashed line), projection layer (yellow dashed line). Note: Images in panels A & C are republished from [30] with permission, however, the presented images show a wider field of view.
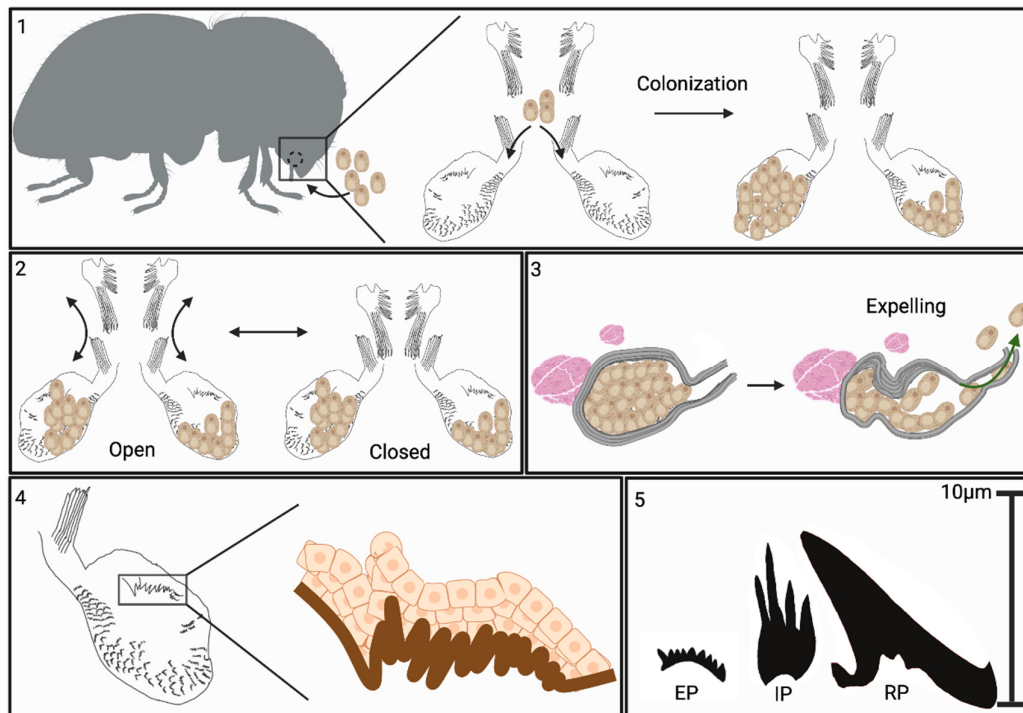
Figure 11. Summary model of *Xyleborus* mycangial features. Box 1: Mycangia structure and colonization: *X. affinis* mycangia are located in the heads of female beetles, just behind and below mandibles, and connected to the pre-oral cavity by narrow entry/exit channels. During feeding, fungal cells are guided into mycangia by long spines at the entrance of channels and opposite the furrows on the labrum. Inside the mycangia, the fungus grows as free-floating yeast-like cells. Box 2: Proposed mechanism of mycangial opening and closing: large spines situated at the roof of the pre-oral cavity, attached to the labrum, are flexed to open/close over the mycangial entrance. Association with projections within mycangia facilitates retention of fungal cells. Box 3: Proposed mechanism of fungal cell expulsion from mycangia: Mycangia are surrounded by dense striated tissue hypothesized to be musculature. Bundles of muscle (fibra) were noted near the ends of mycangia opposite the entry/exit channel. Our data indicate that the mycangia can invaginate, often displaying a pinched end. We hypothesize that the musculature surrounding and adjacent to the mycangia can be flexed, squeezing these organs and facilitating expulsion of fungal cells during inoculation of gallery walls. Box 4: Cellular structures: mycangial wall tissue layers: innermost layer, directly exposed to the mycangia lumen, appears to be a hard sclerotized layer termed the "mycangial inner cuticular layer". From this layer, different projections are noted: Ross projections; large spines present in a cluster near the entrance to the mycangia, tubules, composed of stacked oblong sections, intermediate projections; smaller, thinner, spines which appear to consist of two to three projections originating from a single base and clustering around Ross projections, and eyelash projections; small combs of spines which line the bottom and anterior edges of the interior layer. Surrounding (on the outside) the cuticular layer, are layers of insect epithelial cells (DAPI staining and TEM imaging). Box 5: Projection types described from within mycangia and their relative sizes. EP = eyelash projections, IP = intermediate projections, RP = Ross projections.

4. Discussion

As the ability to "carry" their fungal partners has evolved multiple times independently, the mycangia of ambrosia beetles represent different organs with varying location, development, structure, and selection due to the different paths taken in the course of their evolution [21,34,35]. The majority of Xyleborini genera, as well as some Xyloterini and Ipini species, have evolved a set of two pre-oral mycangia near the esophagus just behind the mandibles and connected to the alimentary canal via either the pre-oral cavity or the pharynx.

Traditional paraffin sectioning, laser ablation tomography (LATscan), and micro-computed tomography (µCT) have been employed to examine oral, pronotal, and mesonotal mycangia in a range of ambrosia beetles [17,20,21,23,24]. The mycangia of *Ambrosiodmus*, *Xylosandrus*, and *Scolytoplatypus* were characterized as being formed of an outer membrane containing the symbiotic fungus, with no glands or secretory cells visible. The mesonotal mycangia of *Xylosandrus compactus* and *X. discolor* have been shown to lie between the pronotum and scutellum, with a single bundle (pronoto-occipitalis) muscle. However, the more recent finer (e.g., via µCT) resolution imaging has shown that in *X. amputatus* this muscle consists of two bundles, each of which splits into four sub-bundles as they cross, with each sub-bundle crossing each other, connecting from the right to the left sides of the scutellum [17]. Additional muscle bundles were found connected to the pronotum posterior. In conjunction with other muscle fibers, longitudinal contraction might constrict these types of mycangia, with deformation of muscle sets posited to occur during gallery excavation [16,17].

A µCT morphological analysis of female *Euwallacea validus* oral paired mycangia (partner fungus, *Fusarium oligoseptatum*) across larval, pupal, and adult stages revealed mycangial organ development during the late pupal stage, with the identification of two sets of mycangia, that could potentially be physically or functionally linked; one termed the superior medial mycangia (consisting of two pouches, located in front of the esophagus and behind the mandible), and the other the inferior, lateral mycangia (also consisting of two pouches, either side of head, behind eyes) [23]. In addition, the resolution of the method allowed for the putative identification of a rudimentary or proto-medial mycangium in males, previously unknown in male Xyleborini.

Confirming previous reports, our data show that the overall structure of the *X. affinis* preoral mycangia consists of two irregular shaped pouch-like organs directly behind and beneath the mandibles and connected to the esophagus via the pre-oral cavity. These pouches appeared to be connected to the mandibular articulations via the entry/exit channel at their frontal end, potentially allowing for their articulation in conjunction with mandibular movements and by mandibular and other sets of muscles. We further elaborate on the entry/exit channels of each mycangium, which appear as furrows with a wider initial segment that narrowed significantly into the mycangium, and were surrounded by dense tissue matter, potentially muscular in nature, but which did not stain with phalloidin. At the mycangial entrance, sets (upper and lower) of long, comb-like spines extending from the labrum or epipharynx "downwards" and from the entrance of the entry/exit channel "upwards" were identified. We hypothesize that these structures, if enervated by muscle tissues and linked to movements of the mandibles, labrum, or epiharynx could act as gates or portcullises to the mycangia, functioning to retain fungal cells during dispersal.

The mycangial envelope itself appeared to have three discernible layers, (from the inside out): (i) a dense staining layer (0.5-2.5 mm) devoid of defined features, but which extended in places into the mycangial lumen forming spines and longer Ross projections. (ii) This was followed by a middle layer of apparent epithelial-like (nucleated) cells (2-5 cells thick), that could also be seen at the base of the spines and projections. (iii) The outermost or peripheral section of the mycangia consisted of a striated layer (1-10 mm, 3-5 bands), which did not appear to be comprised of nucleated cells or actin (i.e., did not stain with DAPI or phalloidin). In posterior sections of mycangia, we consistently noted that this striated layer, and subsequently the mycangial pouch, appeared pinched in appearance, suggesting that this portion of these organs may be flexible, and potentially could be squeezed by surrounding musculature as a mechanism of expelling fungal cells from mycangia during gallery excavation and fungal garden inoculation.

Within or directed into the mycangia from the inner wall, a variety of previously described as well as unreported structures were noted. Larger spines or Ross projections, apparently concentrated in clumps, sometimes, but not always, near or just within the mycangial entrance, have been noted before. The mycangial lumen contained rows of ordered eyelash-like structures lining the inner mycangial wall (here termed eyelash projections). In addition, tubule-like structures consisting of stacked tubes leading to filaments, as well as structures typically with 3-5 filaments of intermediate

size projecting from a diffuse base (intermediate projections), were characterized. Duct-like structures, spines, and hair-like protrusions have been noted for a variety of mycangia, most notably in *Ambrososiophilus atractus*, *Premnobius cavipennis*, *Ambrosiodmus lecontei*, and *E. validus* [22,36,37]. The functions of these enigmatic structures remain to be elucidated, with various hypotheses related to selection and maintenance, coupled with the potential for nutrient and/or signaling exchange, warranting further experimentation. The current work, demonstrating the interior of these structures to contain layers of epithelial cells, indicates dynamic biological functioning beyond inert mechanical retention of fungal cells. Recently, pathways involved in insect tubulogenesis have been implicated in mycangial development [38]. Our observations describe the pre-oral mycangia of a *Xyleborus* ambrosia beetle in unprecedented ultrastructural detail and we propose hypotheses regarding their function as symbiont housing, transporting, and dispensing organs.

References

1. Dzurenko, M.; Hulcr, J. Ambrosia beetles. *Current Biology* **2022**, *32*, R61-R62.

2. Joseph, R.; Keyhani, N. Fungal mutualisms and pathosystems: life and death in the ambrosia beetle mycangia. *Applied Microbiology and Biotechnology* **2021**, *105*, 3393-3410, doi:10.1007/s00253-021-11268-0.

3. Vanderpool, D.; Bracewell, R.R.; McCutcheon, J.P. Know your farmer: Ancient origins and multiple independent domestications of ambrosia beetle fungal cultivars. *Molecular Ecology* **2018**, *27*, 2077-2094, doi:10.1111/mec.14394.

4. Biedermann, P.; Vega, F.; Douglas, A. Ecology and evolution of insect-fungus mutualisms. *Annual Review of Entomology, Vol 65* **2020**, *65*, 431-455, doi:10.1146/annurev-ento-011019-024910.

5. Li, Y.; Bateman, C.; Skelton, J.; Wang, B.; Black, A.; Huang, Y.; Gonzalez, A.; Jusino, M.; Nolen, Z.; Freeman, S.; et al. Preinvasion assessment of exotic bark beetle-vectored fungi to detect tree-killing pathogens. *Phytopathology* **2022**, *112*, 261-270, doi:10.1094/PHYTO-01-21-0041-R.

6. Hulcr, J.; Gomez, D.; Skelton, J.; Johnson, A.; Adams, S.; Li, Y.; Jusino, M.; Smith, M. Invasion of an inconspicuous ambrosia beetle and fungus may affect wood decay in Southeastern North America. *Biological Invasions* **2021**, *23*, 1339-1347, doi:10.1007/s10530-020-02448-6.

7. Dong, Y.; Gao, J.; Hulcr, J. Insect wood borers on commercial North American tree species growing in China: review of Chinese peer-review and grey literature. *Environmental Entomology* **2023**, doi:10.1093/ee/nvad039.

8. Li, Y.; Johnson, A.; Gao, L.; Wu, C.; Hulcr, J. Two new invasive *Ips* bark beetles (Coleoptera: Curculionidae) in mainland China and their potential distribution in Asia. *Pest Management Science* **2021**, *77*, 4000-4008, doi:10.1002/ps.6423.

9. Gomez, D.; Johnson, A.; Hulcr, J. Potential pest bark and ambrosia beetles from Cuba not present in the continental United States. *Florida Entomologist* **2020**, *103*, 96-102, doi:10.1653/024.103.0416.

10. Prior, K.M.; Adams, D.C.; Klepzig, K.D.; Hulcr, J. When does invasive species removal lead to ecological recovery? Implications for management success. *Biological Invasions* **2018**, *20*, 267-283, doi:10.1007/s10530-017-1542-x.

11. Seibold, S.; Muller, J.; Baldrian, P.; Cadotte, M.; Stursova, M.; Biedermann, P.; Krah, F.; Bassler, C. Fungi associated with beetles dispersing from dead wood - Let's take the beetle bus! *Fungal Ecology* **2019**, *39*, 100-108, doi:10.1016/j.funeco.2018.11.016.

12. Skelton, J.; Johnson, A.; Jusino, M.; Bateman, C.; Li, Y.; Hulcr, J. A selective fungal transport organ (mycangium) maintains coarse phylogenetic congruence between fungus-farming ambrosia beetles and their symbionts. *Proceedings of the Royal Society B-Biological Sciences* **2019**, *286*, doi:10.1098/rspb.2018.2127.

13. Carrillo, J.; Rugman-Jones, P.; Husein, D.; Stajich, J.; Kasson, M.; Carrillo, D.; Stouthamer, R.; Eskalen, A. Members of the *Euwallacea fornicatus* species complex exhibit promiscuous mutualism with ambrosia fungi in Taiwan. *Fungal Genetics and Biology* **2019**, *133*, doi:10.1016/j.fgb.2019.103269.

14. Saucedo-Carabez, J.R.; Ploetz, R.C.; Konkol, J.L.; Carrillo, D.; Gazis, R. Partnerships between ambrosia beetles and fungi: lineage-specific promiscuity among vectors of the laurel wilt pathogen, *Raffaelea lauricola*. *Microb Ecol* **2018**, doi:10.1007/s00248-018-1188-y.

15. Kostovcik, M.; Bateman, C.; Kolarik, M.; Stelinski, L.; Jordal, B.; Hulcr, J. The ambrosia symbiosis is specific in some species and promiscuous in others: evidence from community pyrosequencing. *Isme Journal* **2015**, *9*, 126-138, doi:10.1038/ismej.2014.115.

16. Francke-Grossmann, H. Ectosymbiosis in wood-inhabiting insects. In *Symbiosis: Associations of invetebrates birds, ruminants and other biota*, Henry, S.M., Ed.; Academic Press: New York, NY, 1967; Volume II, pp. 142-206.

17. Li, Y.; Ruan, Y.; Kasson, M.; Stanley, E.; Gillett, C.; Johnson, A.; Zhang, M.; Hulcr, J. Structure of the ambrosia beetle (Coleoptera: Curculionidae) mycangia revealed through micro-computed tomography. *Journal of Insect Science* **2018**, *18*, doi:10.1093/jisesa/iey096.

18. Johnson, A.J.; McKenna, D.D.; Jordal, B.H.; Cognato, A.I.; Smith, S.M.; Lemmon, A.R.; Lemmon, E.M.; Hulcr, J. Phylogenomics clarifies repeated evolutionary origins of inbreeding and fungus farming in bark beetles (Curculionidae, Scolytinae). *Mol Phylogenet Evol* **2018**, *127*, 229-238, doi:10.1016/j.ympev.2018.05.028.

19. Batra, L.R. Ambrosia fungi: extent of specificity to ambrosia beetles. *Science* **1966**, *153*, 193-195, doi:10.1126/science.153.3732.193.

20. Mayers, C.G.; Harrington, T.C.; Biedermann, P.H.W. Mycangia define the diverse ambrosia beetle–fungus symbioses. In *The Convergent Evolution of Agriculture in Humans and Insects*, Schultz, T.R., Gawne, R., Peregrine, P.N., Eds.; MIT Press: Cambridge, MA, 2022; pp. 105-142.

21. Mayers, C.; Harrington, T.; Mcnew, D.; Roeper, R.; Biedermann, P.; Masuya, H.; Bateman, C. Four mycangium types and four genera of ambrosia fungi suggest a complex history of fungus farming in the ambrosia beetle tribe Xyloterini. *Mycologia* **2020**, *112*, 1104-1137, doi:10.1080/00275514.2020.1755209.

22. Li, Y.; Simmons, D.R.; Bateman, C.C.; Short, D.P.G.; Kasson, M.T.; Rabaglia, R.J.; Hulcr, J. New fungus-insect symbiosis: culturing, molecular, and histological methods determine saprophytic Polyporales mutualists of *Ambrosiodmus* ambrosia beetles. *Plos One* **2015**, *10*, doi:ARTN e0137689 10.1371/journal.pone.0137689.

23. Spahr, E.; Kasson, M.; Kijimoto, T. Micro-computed tomography permits enhanced visualization of mycangia across development and between sexes inEuwallaceaambrosia beetles. *Plos One* **2020**, *15*, doi:10.1371/journal.pone.0236653.

24. Jiang, Z.R.; Kinoshita, S.; Sasaki, O.; Cognato, A.I.; Kajimura, H. Non-destructive observation of the mycangia of *Euwallacea interjectus* (Blandford) (Coleoptera: Curculionidae: Scolytinae) using X-ray computed tomography. *Entomological Science* **2019**, *22*, 173-181.

25. Ploetz, R.C.; Hulcr, J.; Wingfield, M.J.; de Beer, Z.W. Destructive tree diseases associated with ambrosia and bark beetles: black swan events in tree pathology? *Plant Disease* **2013**, *97*, 856-872, doi:10.1094/Pdis-01-13-0056-Fe.

26. Ploetz, R.C.; Konkol, J.L.; Narvaez, T.; Duncan, R.E.; Saucedo, R.J.; Campbell, A.; Mantilla, J.; Carrillo, D.; Kendra, P.E. Presence and prevalence of *Raffaelea lauricola*, cause of laurel wilt, in different species of ambrosia beetle in Florida, USA. *J Econ Entomol* **2017**, doi:10.1093/jee/tow292.

27. Pena, J.E.; Carrillo, D.; Duncan, R.E.; Capinera, J.L.; Brar, G.; Mclean, S.; Arpaia, M.L.; Focht, E.; Smith, J.A.; Hughes, M.; et al. Susceptibility of *Persea* spp. and other Lauraceae to attack by redbay ambrosia beetle, *Xyleborus glabratus* (Coleoptera: Curculionidae: Scolytinae). *Florida Entomologist* **2012**, *95*, 783-787, doi:Doi 10.1653/024.095.0334.

28. Fraedrich, S.W.; Harrington, T.C.; Rabaglia, R.J.; Ulyshen, M.D.; Mayfield, A.E.; Hanula, J.L.; Eickwort, J.M.; Miller, D.R. A fungal symbiont of the redbay ambrosia beetle causes a lethal wilt in redbay and other Lauraceae in the Southeastern United States. *Plant Disease* **2008**, *92*, 215-224, doi:10.1094/Pdis-92-2-0215.

29. Saucedo, J.R.; Ploetz, R.C.; Konkol, J.L.; Angel, M.; Mantilla, J.; Menocal, O.; Carrillo, D. Nutritional symbionts of a putative vector, *Xyloborus bispinatus*, of the laurel wilt pathogen of avocado, *Raffaelea lauricola*. *Symbiosis* **2017**, 1-10, doi:10.1007/s13199-017-0514-3.

30. Joseph, R.; Bansal, K.; Keyhani, N.O. Host switching by an ambrosia beetle fungal mutualist: Mycangial colonization of indigenous beetles by the invasive laurel wilt fungal pathogen. *Environ Microbiol* **2023**, *25*, 1894-1908, doi:10.1111/1462-2920.16401.

31. Menocal, O.; Cruz, L.F.; Kendra, P.E.; Berto, M.; Carrillo, D. Flexibility in the ambrosia symbiosis of *Xyleborus bispinatus*. *Front Microbiol* **2023**, *14*, 1110474, doi:10.3389/fmicb.2023.1110474.

32. Cruz, L.F.; Menocal, O.; Mantilla, J.; Ibarra-Juarez, L.A.; Carrillo, D. Xyleborus volvulus (Coleoptera: Curculionidae): Biology and Fungal Associates. *Appl Environ Microbiol* **2019**, *85*, doi:10.1128/AEM.01190-19.

33. Zhou, Y.; Lu, D.; Joseph, R.; Li, T.; Keyhani, N. High efficiency transformation and mutant screening of the laurel wilt pathogen, *Raffaelea lauricola*. *Applied Microbiology and Biotechnology* **2020**, *104*, 7331-7343, doi:10.1007/s00253-020-10762-1.

34. Jiang, Z.-R.; Kinoshita, S.; Sasaki, O.; Cognato, A.I.; Kajimura, H. Non-destructive observation of the mycangia of *Euwallacea interjectus* (Blandford) (Coleoptera: Curculionidae: Scolytinae) using X-ray computed tomography. *Entomological Science* **2019**, *22*, 173-181.

35. Spahr, E.; McLaughlin, S.; Tichinel, A.; Kasson, M.; Kijimoto, T. Staining and scanning protocol for micro-computed tomography to observe the morphology of soft tissues in ambrosia beetles. *Bio-Protocol* **2023**, *13*, doi:10.21769/BioProtoc.4584.

36. Bateman, C.; Huang, Y.T.; Simmons, D.R.; Kasson, M.T.; Stanley, E.L.; Hulcr, J. Ambrosia beetle Premnobius cavipennis (Scolytinae: Ipini) carries highly divergent ascomycotan ambrosia fungus, Afroraffaelea ambrosiae gen. nov et sp nov (Ophiostomatales). *Fungal Ecology* **2017**, *25*, 41-49, doi:10.1016/j.funeco.2016.10.008.

37. Kasson, M.T.; Wickert, K.L.; Stauder, C.M.; Macias, A.M.; Berger, M.C.; Simmons, D.R.; Short, D.P.G.; DeVallance, D.B.; Hulcr, J. Mutualism with aggressive wood-degrading Flavodon ambrosius (Polyporales) facilitates niche expansion and communal social structure in Ambrosiophilus ambrosia beetles. *Fungal Ecology* **2016**, *23*, 86-96, doi:10.1016/j.funeco.2016.07.002.

38. Spahr, E.J.; Wasef, F.; Kasson, M.T.; Kijimoto, T. Developmental genetic underpinnings of a symbiosis-associated organ in the fungus-farming ambrosia beetle Euwallacea validus. *Sci Rep* **2023**, *13*, 14014, doi:10.1038/s41598-023-40296-1.